JOURNAL OF BACTERIOLOGY, July 1996, p. 3877–3884 Vol. 178, No. 13
0021-9193/96/$04.00+0

FtsZ Ring Formation in *fts* Mutants

STEPHEN G. ADDINALL, ERFEI BI,† AND JOE LUTKENHAUS*

Department of Microbiology, Molecular Genetics and Immunology, University of Kansas Medical Center, Kansas City, Kansas 66160

Received 13 February 1996/Accepted 26 April 1996

The formation of FtsZ rings (Z rings) in various *fts* mutants was examined by immunoelectron microscopy and immunofluorescence. In two temperature-sensitive *ftsZ* mutants which form filaments with smooth morphology, the Z ring was unable to form. In *ftsA*, *ftsI*, and *ftsQ* mutants, which form filaments with an indented morphology, Z rings formed but their contraction was blocked. These results indicate that fully functional *ftsA*, *ftsQ*, and *ftsI* genes are not required for Z-ring formation and are unlikely to have a role in localization of the Z ring. The results also suggest that one function of the Z ring is to localize the activity of other *fts* gene products.

It has been demonstrated by immunoelectron microscopy that FtsZ undergoes dynamic localization during the cell division cycle in both *Escherichia coli* and *Bacillus subtilis* (2, 29). In these organisms, FtsZ migrates from the cytoplasm to midcell, where it is localized in a ring pattern designated the FtsZ ring (Z ring). It appears that once the Z ring is formed, septation ensues, with the Z ring maintaining a position at the leading tip of the invaginating septum. Upon completion of the septum, FtsZ disassembles and is not associated with the nascent cell pole. It has been hypothesized that the Z ring functions as a cytoskeletal element that mediates invagination of the septum (20). In vitro evidence demonstrating that FtsZ is a GTPase (12, 22, 25, 29) and can under go GTP-dependent assembly into filaments is also consistent with this hypothesis (7, 14, 23). Also consistent with this hypothesis is our finding that Z rings with abnormal geometries are formed in an *ftsZ26*(Ts) mutant (3). Such abnormal Z rings are associated with abnormal septal morphologies, suggesting that the pattern of septal ingrowth is dictated by the shape of the Z ring.

In addition to *ftsZ*, a number of additional genes have been identified that are required for cell division. Among the best characterized are *ftsA*, *ftsQ*, and *ftsI*. *ftsI* encodes PBP3, which is specifically required for septal peptidoglycan biosynthesis (6, 26). Presumably, this enzyme is locally activated during septation. *ftsA* encodes a protein that has homology to the DnaK-actin family of ATPases (5). Little is known about the function of FtsQ (8).

The order in which the various genes function during cell division is suggested by the morphology of the filaments produced as a result of loss of the gene function (27). A temperature-sensitive mutation in *ftsZ* produces filaments with a smooth morphology, whereas mutations in *ftsA* and *ftsI* produce filaments with indented morphology. These indentations are thought to arise from abortive septation events, indicating that *ftsA* and *ftsI* act after *ftsZ*. This order of action of these genes agrees with the order that has been inferred from the terminal phenotype observed after combining a temperature-sensitive division mutation with a mutation in the peptidoglycan elongation system which causes *E. coli* to grow as spheres (1). The addition of such a spherical mutation amplifies the effect of septation on morphology. Thus, combination of *ftsZ84* with a *rodA* mutation results in lemon-shaped cells with no sign of initiation of septation at the nonpermissive temperature. In contrast, combination of a *rodA* mutation with a *ftsA*, *ftsI*, or *ftsQ* mutation results in filaments that appear to have partial constrictions, indicating that septation initiated but was then aborted.

From the above analysis of the order of gene action, one would predict that the Z ring can form in *ftsA*, *ftsI*, and *ftsQ* mutants and initiates septation. However, progression is blocked and the Z rings may or may not be stable. In *ftsZ* mutants, the Z ring either does not form or, if it does, does not function. To test these expectations, we examined Z-ring formation in these mutants by using immunoelectron microscopy and immunofluorescence.

MATERIALS AND METHODS

Bacterial strains. The strains used in this study are all derivatives of *E. coli* K-12 strain MC4100 (2, 9). They included MC4100T (*leu*::Tn*10*), MCZ84 [*leu*::Tn*10 ftsZ84* (Ts)], MCZ26 [*leu*::Tn*10 ftsA27* (Ts)], MCA6 [*leu*::Tn*10 ftsA6* (Ts)], MCA12 [*leu*::Tn*10 ftsA12* (Ts)], MCA27 [*leu*::Tn*10 ftsZ84* (Ts)], MCQ1 [*leu*::Tn*10 ftsQ1* (Ts)], and MCI23 [*leu*::Tn*10 ftsI23* (Ts)] and were described previously (3, 11).

All strains were grown in L broth as previously described (2, 11).

Immunoelectron microscopy. The procedure used for immunoelectron microscopy was essentially that described previously (2). Exponentially growing cells were fixed in the growth medium by addition of 2% glutaraldehyde for 30 to 45 min. Cells were collected by centrifugation, and the pellet was washed once with PBS (10 mM Na_3PO_4 [pH 7.4], 150 mM NaCl, 15 mM KCl) and then immersed in 30% ethanol for 20 min. Cells were stained for 17 min in 2% uranyl acetate dissolved in 50% ethanol. The cells were subsequently dehydrated by incubation for 5 min each in a series of ethanol solutions with increasing concentrations of 70, 80, 90, and 100%. Incubation in 100% ethanol was repeated once for 10 min. Cells were infiltrated with LR White resin (London Resin Co.) overnight at 4°C and embedded by addition of fresh resin and incubation overnight at 60°C. Thin sections were cut with an LKB-Ultratome (NOVA) and placed on nickel grids for immunostaining. The grids were rinsed in 0.2 M Tris-HCl (pH 7.6) for 5 min, blocked in 50 mM Tris-HCl–0.15 M NaCl–1% bovine serum albumin (BSA) (TSB buffer) for 15 min, and stained with an affinity-purified FtsZ antibody solution (in TSB buffer) for 1 to 2 h at room temperature. The grids were washed twice with TSB buffer and incubated with 10-nm gold-labeled goat anti-rabbit immunoglobulin G (Amersham; diluted 1:10 in TSB buffer) for 1.5 h at room temperature. The grids were again washed twice with TSB buffer and then twice with distilled water. Cells were stained for 2 min with aqueous 7% uranyl acetate and dried before examination with an electron microscope (JEOL 100-CXII).

Immunofluorescent staining. Cells were fixed and stained by minor adjustments to a protocol provided by Kit Pogliano (16). Derivatives of strain MC4100 growing at 30 or 42°C were fixed directly in growth medium by addition of paraformaldehyde, glutaraldehyde, and Na_3PO_4 buffer (pH 7.4) to final concentrations of 2.6% (vol/vol), 0.04% (vol/vol), and 32.25 mM, respectively. The mixture was incubated for 10 min at room temperature and for a further 50 min on ice. Fixed cells were washed three times in PBS at room temperature by

* Corresponding author. Phone: (913) 588-7054. Fax: (913) 588-7295. Electronic mail address: jlutkenh@kumc.edu.

† Present address: Department of Biology, University of North Carolina, Chapel Hill, NC 27599.

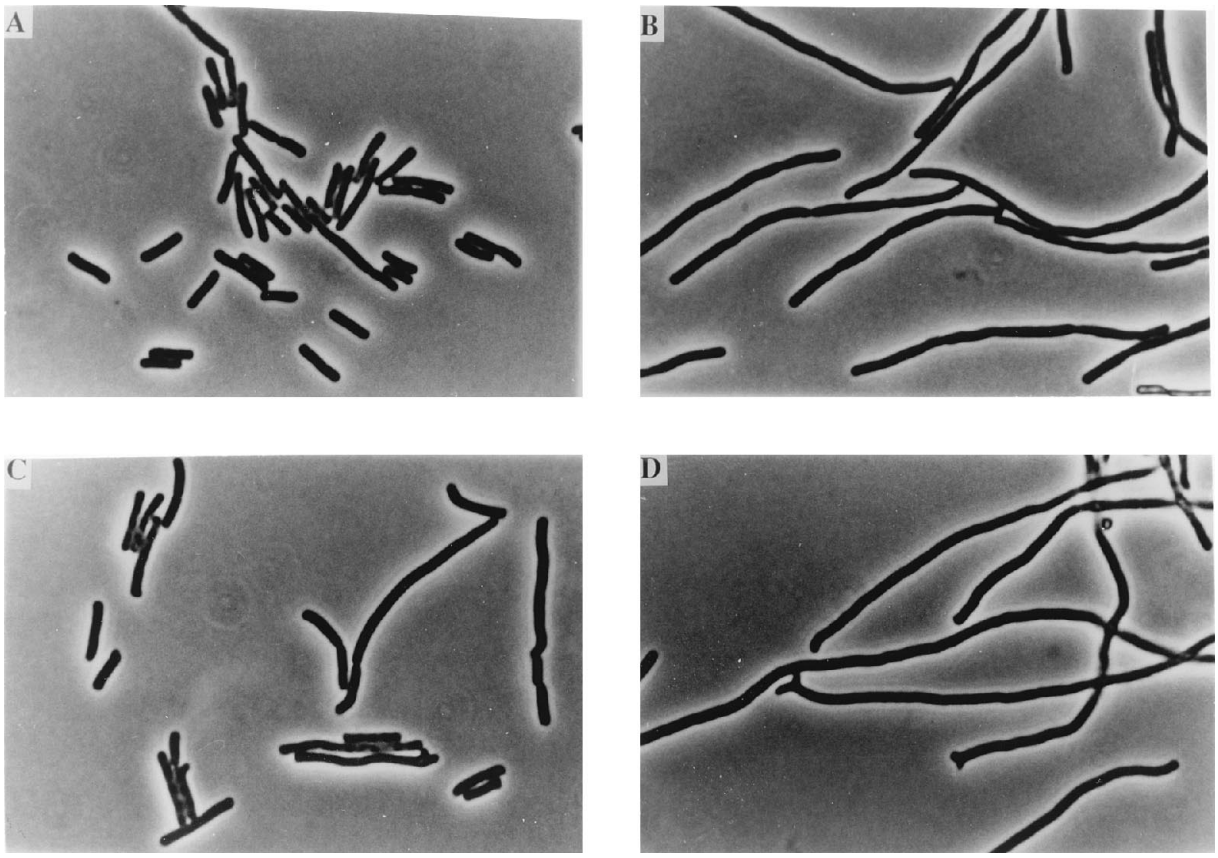

FIG. 1. Morphology of filaments. Strain MCA27 [*ftsA27*(Ts)] and MCZ26 [*ftsZ26*(Ts)] cells growing exponentially at 30°C (A and C, respectively) were shifted to 42°C for 45 min (B and D, respectively) and photographed. Some indentations are visible along the length of the *ftsA* mutant filaments but not along the *ftsZ* mutant filaments.

centrifugation and then resuspended in GTE (50 mM glucose, 10 mM EDTA, 20 mM Tris [pH 7.5]). Freshly prepared lysozyme (Sigma) in GTE was added to the fixed cells to a final concentration of 4 to 20 μg/ml. Cells were immediately transferred to the wells of a multiwell microscope slide (ICN Biochemicals) pretreated with poly-L-lysine (0.1% [wt/vol]; Sigma), and the permeabilization was continued for 1 min. The optimal concentration of lysozyme was determined for each strain. Also, fixed cells resuspended in GTE could be stored for a number of days at 4°C before lysozyme treatment. Stored cells required a lower concentration of lysozyme for optimal results than if they had been used immediately. Liquid was aspirated from the wells, and each well was washed twice with PBS and then left to air dry completely. Permeabilized cells were rehydrated for 4 min by addition of 10 μl of PBS to each well. This was then replaced by 10 μl of blocking solution (2% [wt/vol] BSA in PBS [BSA-PBS]), and the slides were incubated for 10 to 15 min at room temperature. The blocking solution was replaced with 10 μl of a 1:250 dilution (in BSA-PBS) of an affinity-purified rabbit polyclonal antibody to *E. coli* FtsZ (2). Incubation with the primary antibody was continued overnight at 4°C, after which wells were washed 10 times with PBS. The secondary antibody—10 μl of a 1:100 dilution (in BSA-PBS) of a Cy3-conjugated anti-rabbit immunoglobulin G antibody (0.75 mg/ml; Jackson Immunoresearch)—was added, and incubation was carried out for 1 to 3 h in the dark at room temperature. Incubation for 1 h seemed to give the best signal-to-background ratio, but often this was too faint for photography and longer times were used. Wells were washed 10 times with PBS and once with SlowFade Equilibration Buffer (Molecular Probes), and then the slide was mounted in SlowFade (8 μl per well; Molecular Probes) and stored at −20°C until microscopic observation. An extra wash with SlowFade Equilibration Buffer containing 4′,6-diamidino-2-phenylindole (DAPI; 1.5 μg/ml) was included after the PBS washes for observation of DNA.

Samples were observed and photographed with a Nikon Optiphot fluorescence microscope equipped with an E Plan oil immersion lens (Nikon) with a 100× objective and a Contax 167MT camera. Fluorescence was observed by using a 460- to 490-nm excitation filter and a 520-nm barrier filter (B-2A; Nikon). Fluorescence and phase-contrast photographs were obtained with Kodak Ektachrome 400 slide film or Kodak Tmax 400 print film. Images were scanned from slides with a Nikon LS-3510 AF slide scanner and imported into Adobe Photoshop software. Scoring of cells for fluorescence was performed with color slides or black-and-white prints or by direct viewing under a microscope.

RESULTS

Localization of FtsZ by immunoelectron microscopy. By utilizing immunoelectron microscopy, we examined the location of FtsZ in various *fts* mutants. The first mutants that we examined included two temperature-sensitive *ftsZ* mutants, the *ftsZ84* and *ftsZ26* mutants. Both of these mutants are blocked in cell division at the nonpermissive temperature and produce filaments with a smooth morphology [Fig. 1C and D; the *ftsZ26*(Ts) mutant is shown]. Examination of cells at the permissive temperature revealed that FtsZ, as indicated by the clustering of gold particles, was localized to the leading edge of the septum (data not shown), as previously reported for wild-type cells and for the *ftsZ26*(Ts) mutant (2, 3). After 45 min at the nonpermissive temperature, filaments were fixed and stained. Numerous filaments were examined by immunoelectron microscopy, and an example of an *ftsZ26*(Ts) mutant is shown in Fig. 2. Because of the length of the filaments, it was difficult to view entire filaments and so only portions of filaments were observed. In all cases, the distribution of gold particles appeared to be quite random in the cytoplasm and in no instances were clusters of gold particles observed at the cell membrane directly across from each other. The same results were obtained with the *ftsZ84*(Ts) mutant (data not shown).

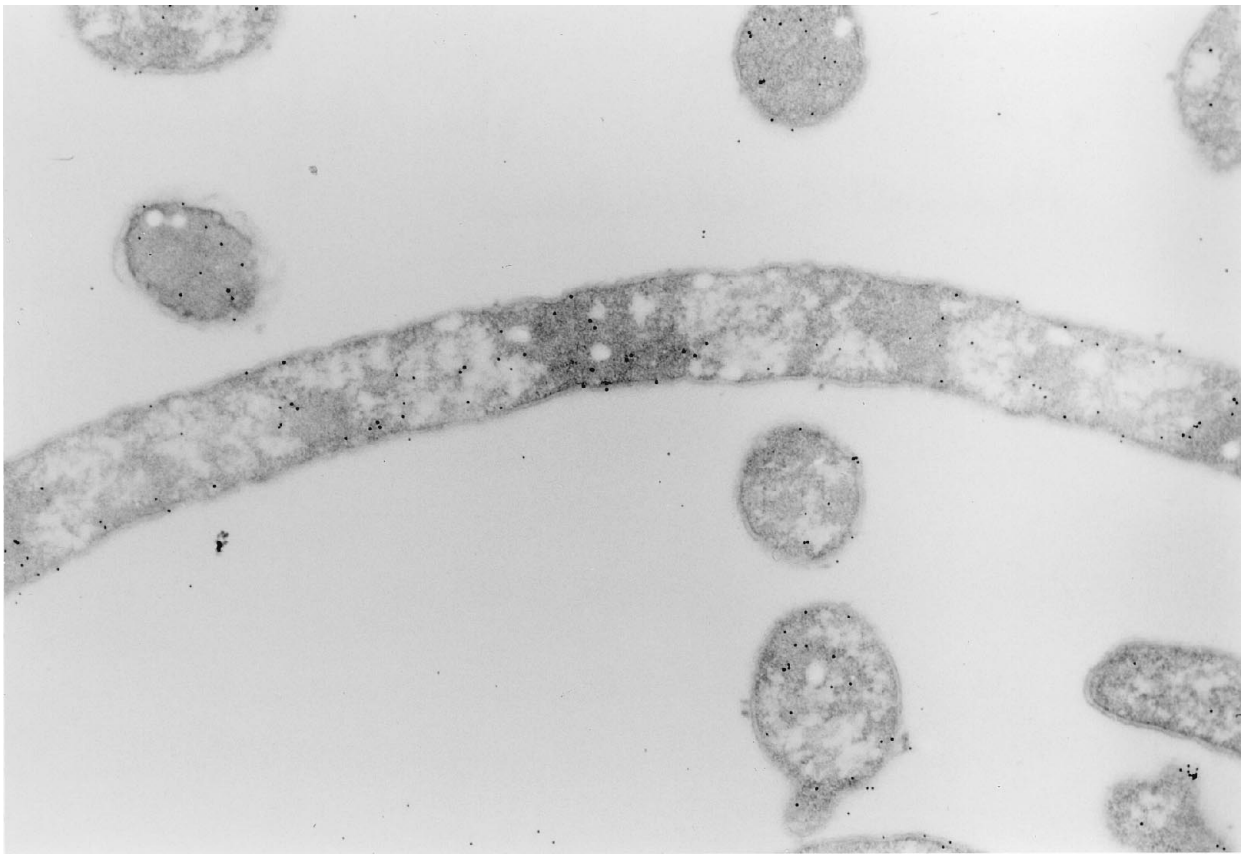

FIG. 2. Immunolocalization of FtsZ in the *ftsZ26*(Ts) mutant strain. FtsZ was localized by immunoelectron microscopy in MCZ26 cells that had been shifted to 42°C for 45 min.

These results indicate that the these mutant FtsZ proteins are unable to localize at the nonpermissive temperature.

We next examined *ftsA* mutants. The *ftsA12*(Ts), *ftsA27*(Ts), and *ftsA6*(Ts) mutants were examined. After 45 min at the nonpermissive temperature, each of these mutants produced filaments with indented morphology [Fig. 1A and B; the *ftsA27*(Ts) mutant is shown]. At the permissive temperature, each septum was decorated with gold particles, indicating that the Z ring was present [Fig. 3A; the *ftsA27*(Ts) mutant is shown]. Many filaments of each mutant at the nonpermissive temperature were examined, and an example is shown in Fig. 3B. This filament was fairly typical of those observed. At least two indentations were visible along the length of the filament. One of these indentations was symmetrically decorated with gold particles, whereas the other was not. It was difficult to estimate the fraction of indentations that were labeled, as they

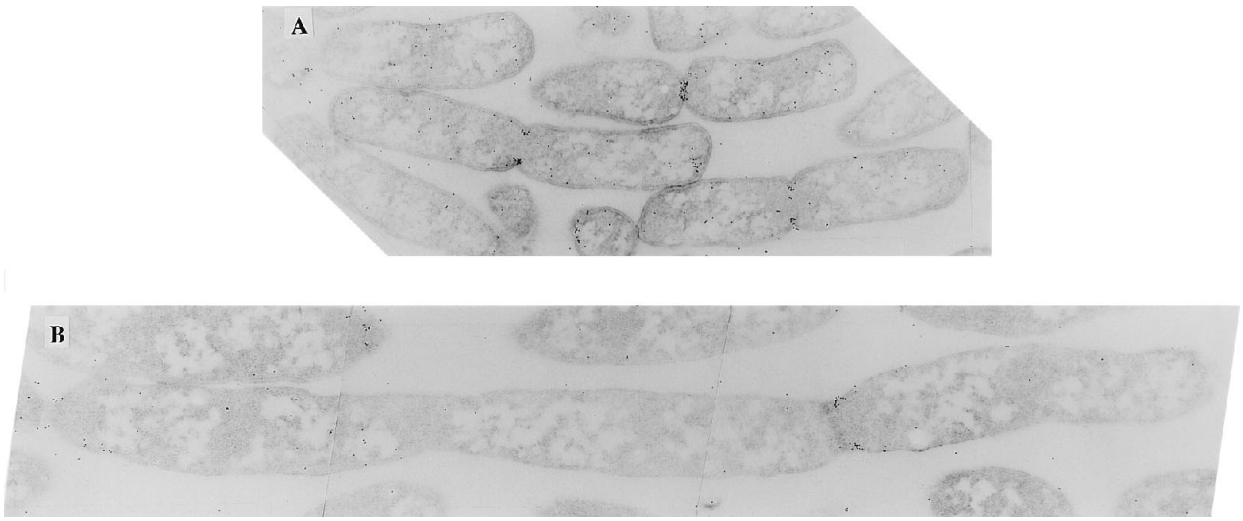

FIG. 3. Immunolocalization of FtsZ in the *ftsA27*(Ts) mutant strain. (A) MCA27 grown at 30°C. (B) MCA27 45 min after a shift to 42°C.

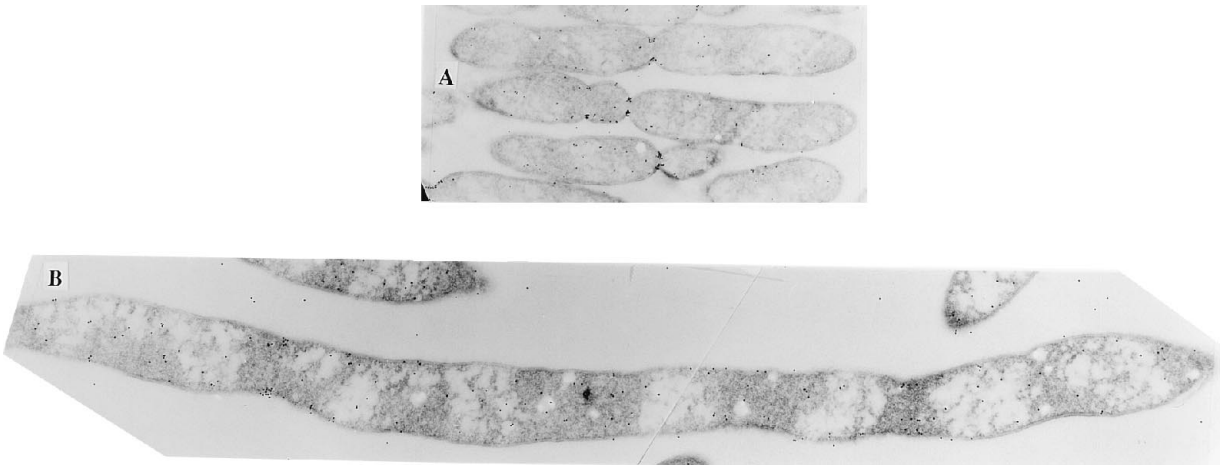

FIG. 4. Immunolocalization of FtsZ in the *ftsI23*(Ts) mutant strain. (A) MCI23 grown at 30°C. (B) MCI23 45 min after a shift to 42°C.

appeared more regular and obvious with the light microscope than with the electron microscope. Careful examination with the light microscope revealed that although the filaments had an indented morphology, the indentations were variable in frequency and spacing. In any event, some of the indentations were decorated with gold particles but others were not. One *ftsI* mutant, the *ftsI23*(Ts) mutant, was also examined (Fig. 4). The results were the same as those obtained with the *ftsA* mutants.

Although the results obtained with the *ftsZ* mutants are relatively easy to interpret, those obtained with the *ftsA* and *ftsI* mutants are more difficult to interpret. With the two *ftsZ* mutants, the Z ring was unable to form at the nonpermissive temperature. However, with the *ftsI* and *ftsA* mutants, the situation is less clear. Although some apparently abortive septa were symmetrically decorated with gold particles, others were not. Thus, it is not clear if the decorated indentations indicate septa initiated before the temperature shift or after.

Localization of FtsZ by immunofluorescence. Recently, immunofluorescence has been applied to bacteria to localize proteins (16, 21). This technique offers several advantages over immunoelectron microscopy, although there is a loss of resolution. The major advantages include relative ease of sample preparation, increased sensitivity, the ability to view whole cells, and the ability to look at large numbers of cells.

To initiate experiments with this technique, we examined cells of wild-type strain MC4100T grown at 30°C in L broth. Cells were fixed in the growth medium and processed for immunofluorescence as described in Materials and Methods. Examination of such fixed cells by phase-contrast microscopy and immunofluorescence revealed that most cells in the population had a single bright band at the cell center indicating the location of FtsZ (Fig. 5). Counting of over 900 cells revealed that 92% had FtsZ localized at the longitudinal midpoint of the cell. No cells with more than one immunofluorescent band were observed. Cells that did not display an immunofluorescent band were the smallest cells in the population, indicating that they were newborn cells (Fig. 5, arrow 3). In stained cells, the diameter (since it is a ring) of the immunofluorescent band corresponded to the extent to which septation had progressed; in cells in which septation was nearly complete, the immunofluorescence was localized to a dot at the septum (compare the bands indicated by arrows 1 and 2 in Fig. 5). This decrease in the diameter of the fluorescently stained band in *E. coli* has also been observed by Levin and Losick (19). These results indicated that immunofluorescent labeling worked very well for localization of FtsZ, and the results are very similar to those obtained by immunoelectron microscopy that were reported earlier (2). The only difference is that more cells were shown to contain a Z ring by this technique, indicating that immunofluorescence is more sensitive. Interestingly, the fraction of cells that contain a Z ring is very similar to the number

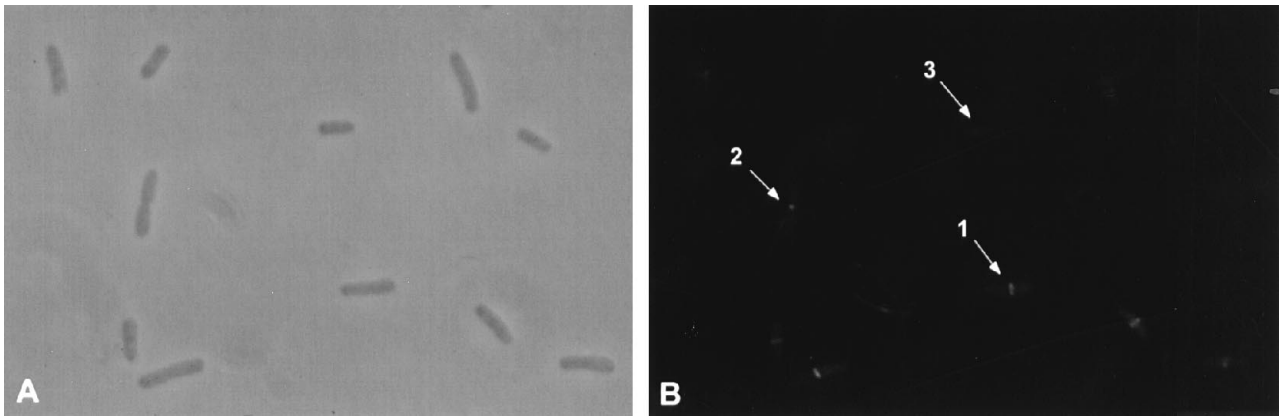

FIG. 5. Localization of FtsZ by immunofluorescence. Exponentially growing strain MC4100T cells were processed for staining with antibodies to FtsZ as described in Materials and Methods. (A) Phase-contrast photomicrograph. (B) Fluorescence photomicrograph of the same field as in panel A.

of cells that contain segregated nucleoids (~80%), and when cells were examined simultaneously for DNA distribution and FtsZ localization, the Z ring was always found to correspond to a gap between two nucleoids (data not shown).

Since immunofluorescence is more sensitive than immunoelectron microscopy, it was of interest to reexamine FtsZ localization in the *ftsZ84*(Ts) and *ftsZ26*(Ts) mutants at the nonpermissive temperature. Cells from an *ftsZ84*(Ts) mutant culture growing at 30°C and 30 and 45 min after a shift to 42°C were fixed and stained. No bright fluorescent bands were detected at either time point at 42°C, whereas most of the cells in the 30°C culture contained a bright midcell band. To illustrate this point, fixed cells from the 30°C culture were mixed with fixed cells from the culture shifted to 42°C for 45 min and stained. Figure 6A and B, phase-contrast and fluorescence photomicrographs, respectively, show a short cell from the 30°C culture and a filament from the 42°C culture. The cell from the 30°C culture had a single immunofluorescent midcell band, whereas the long filament from the 42°C culture displayed only diffuse staining. The diffuse staining in the filament was similar to that observed in a control experiment, in which antibody to a protein (GroEL) not expected to be specifically localized in the cell was used with wild-type cells (data not shown). These results confirm those obtained with immunoelectron microscopy, which indicated the absence of Z rings. However, with the more sensitive immunofluorescence technique, we were able to examine a large number of complete filaments, providing more confidence in the result. The same results were obtained with the *ftsZ26*(Ts) mutant at 42°C (data not shown).

Next we examined FtsZ localization in other *fts* mutants (Fig. 6C to H). Those examined included the *ftsQ1*(Ts), *ftsA12* (Ts), and *ftsI23*(Ts) mutants. The results are presented as photographs of individual cells and graphs that summarize data collected from large numbers of cells fixed at 30°C and at 30 and 45 min after a shift to the nonpermissive temperature. Figure 6C and D, E, and F, and G and H show phase-contrast and immunofluorescence photomicrographs of stained filaments from *ftsQ1*(Ts), *ftsA12*(Ts), and *ftsI23*(Ts) mutant cultures, respectively. These photographs reveal that filaments formed as a result of either of these mutations had a number of Z rings, as indicated by the bright fluorescent bands visible at fairly regular intervals along the length of the filaments. Thus, the first conclusion is that Z rings are formed after the temperature shift. This is shown in Fig. 7, which presents data from an analysis of large numbers of cells. For each of the mutants grown at 30°C, the histograms show that most of the cells contained a single Z ring; however, some cells with no rings and some with more than one ring were observed. With the *ftsA12*(Ts) and *ftsQ1*(Ts) mutants, 15 and 20% of the cells, respectively, had two rings (at 1/4 and 3/4 of the cell length) that symmetrically flanked a midcell indentation. Interestingly, in the wild-type strain, no cells with more than one ring were observed, indicating that in these mutants, regulation of the Z ring is already affected at the permissive temperature. In these same graphs, data are presented that were collected at two times, 30 and 45 min, after the shift for each of the mutants. The results for all of the mutants are similar. In the 30-min culture, the most frequently observed class contained cells with two rings and there were many cells with more than two rings. At 45 min, the most frequently observed class contained cells with three or four rings and there were also many cells with more rings. For the *ftsI23*(Ts) mutant, the average number of rings per cell increased from 1.07 at 30°C to 2.17 at 30 min after the temperature shift and 3.26 at 45 min after the temperature shift. A slightly larger increase was seen in the *ftsA12*(Ts) mutant, and a slightly smaller increase was seen in the *ftsQ1*(Ts) mutant. Also apparent from the graphs is the heterogeneity in the populations. For example, with each mutant strain after 45 min there were cells with no rings, as well as many cells with more than 2 rings (up to 12 rings in some cells).

DISCUSSION

Several conclusions can be drawn from the results presented in this report. First, the temperature-sensitive FtsZ mutant proteins FtsZ84 and FtsZ26 are unable to form a Z ring at the nonpermissive temperature. Second, the Z ring can form in the absence of functional *ftsA*, *ftsI*, and *ftsQ* genes, indicating that these genes function after *ftsZ*, as previously concluded (1), and are unlikely to be required for Z-ring formation.

Previous work had separated division mutants into two classes based on cell morphology (1, 27). In one class, *ftsZ* mutants, division appeared to be blocked early and filaments had a smooth morphology or a lemon morphology when combined with a mutation that caused cells to grow as spheres. In a second class, including the *ftsA*, *ftsI*, and *ftsQ* mutants, division appeared to be blocked at a later step as filaments had an indented morphology or sausage-like appearance when combined with a spherical mutation. Judging from our results, this distinction correlates with the ability of mutants to form a Z ring. Thus, the smooth morphology corresponds to the absence of rings and the indented morphology is seen with mutants that are able to form rings. This result also extends to various inhibitors. Thus, SulA production, which blocks cell division (17), producing smooth filaments, or lemons in the presence of a spherical mutation (1), has been shown to block Z-ring formation (4). We have confirmed that result by using the more sensitive immunofluorescence technique (data not shown). Also, overproduction of MinCD, which gives a smooth morphology, blocks formation of Z rings (4).

Before discussing Z-ring formation in the various mutants, it is worth discussing the results obtained with wild-type cells. We observed that 92% of the cells in a wild-type population growing in rich medium had a Z ring. The ring was always at midcell, and never was more than one ring per cell observed in viewing thousands of cells. The percentage of cells with a ring was somewhat higher than expected upon the basis of an earlier study utilizing immunoelectron microscopy (2). In that study, cells with an invagination were always observed to have a Z ring but cells without an invagination only rarely had a Z ring. Since about 45% of the cells growing under those conditions had a visible invagination, the fraction that would be expected to have a Z ring would be only slightly higher. The 92% positive cells seen in this study is a much higher percentage, even though we also observed about 45% of the cells with a constriction (data not shown). We think this is largely due to the greater sensitivity of the immunofluorescence technique.

Importantly, this study confirmed that the Z ring forms before there is a visible invagination, as concluded previously (2). Thus, at this growth rate, a Z ring is formed shortly after division and there is only a small gap in the cell cycle when a Z ring is not present. The time from appearance of the Z ring to visible invagination may indicate the time necessary for the Z ring to mature into a fully active divisome (2, 24) by addition of other Fts proteins.

Our results indicate that cells grown in rich medium with a fast doubling time form a Z ring just a few minutes after division. For cells at such a fast growth rate, the appearance of the Z ring coincides with the separation of nucleoids which also occurs shortly after division (as a prelude to the next

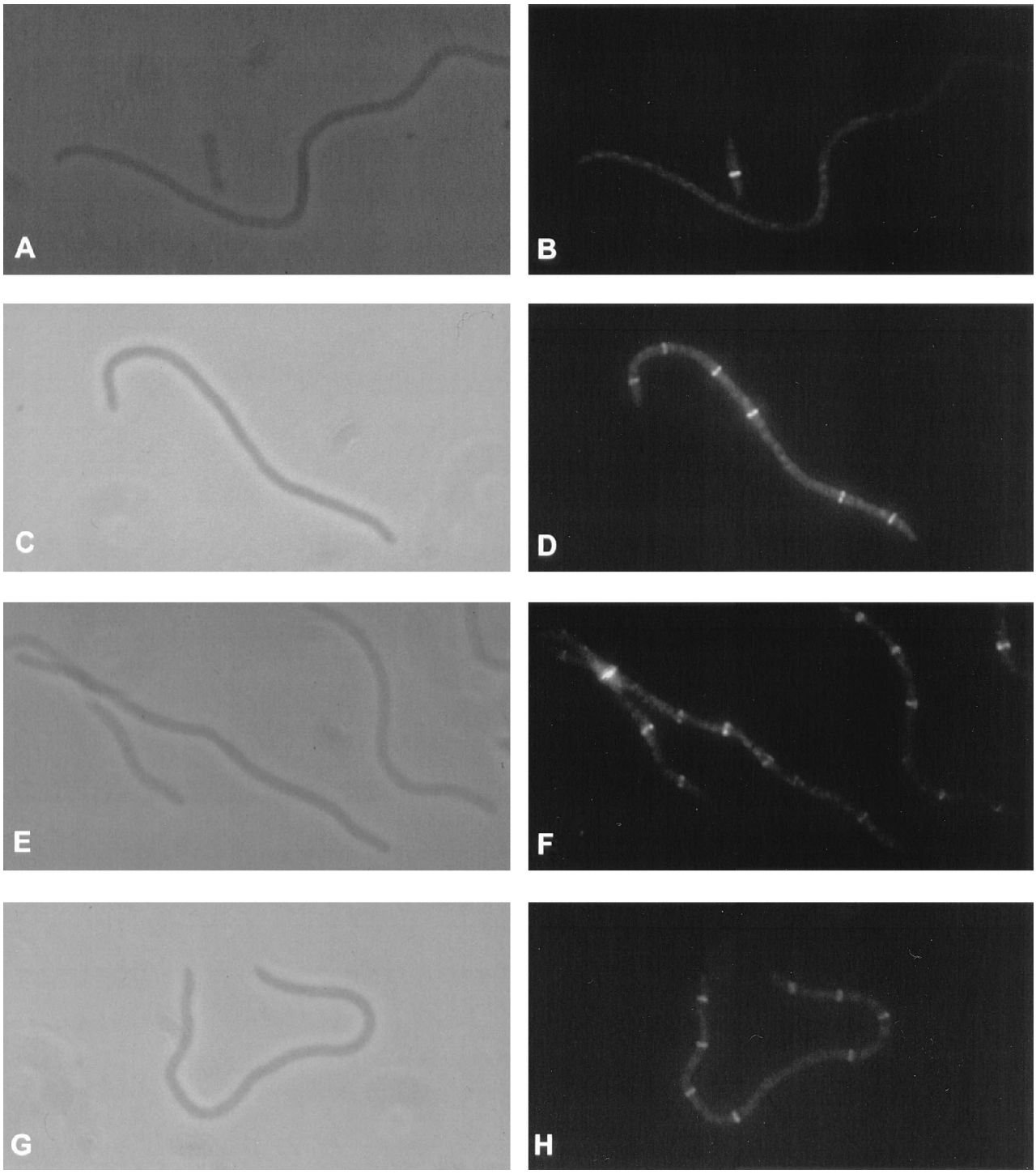

FIG. 6. FtsZ localization in *fts* mutants. A, C, E, and G, phase-contrast photomicrographs; B, D, F, and H, immunofluorescence photomicrographs. Cells from the *ftsZ84*(Ts) strain growing at 30°C and 45 min after a shift to 42°C were fixed and then mixed before staining. Photomicrographs A and B contain a relatively short cell from the 30°C culture and a long filament from the 42°C culture. For the other mutants, only cells from the 42°C culture are shown. C and D, *ftsA12*(Ts); E and F, *ftsQ1*(Ts); G and I, *ftsI23*(Ts).

division). Whether nucleoid segregation or termination of DNA replication, which occurs immediately before partition, acts as a signal is not clear. However, throughout our experiments, we have observed Z rings only between separated nucleoids, suggesting that the Z ring is localized only between segregated nucleoids under these conditions (including filamentation).

As stated above, the ability of FtsZ to localize in *ftsA12*(Ts), *ftsI23*(Ts), and *ftsQ1*(Ts) mutants is consistent with the previous notion that these genes function after *ftsZ* (1, 27). Our

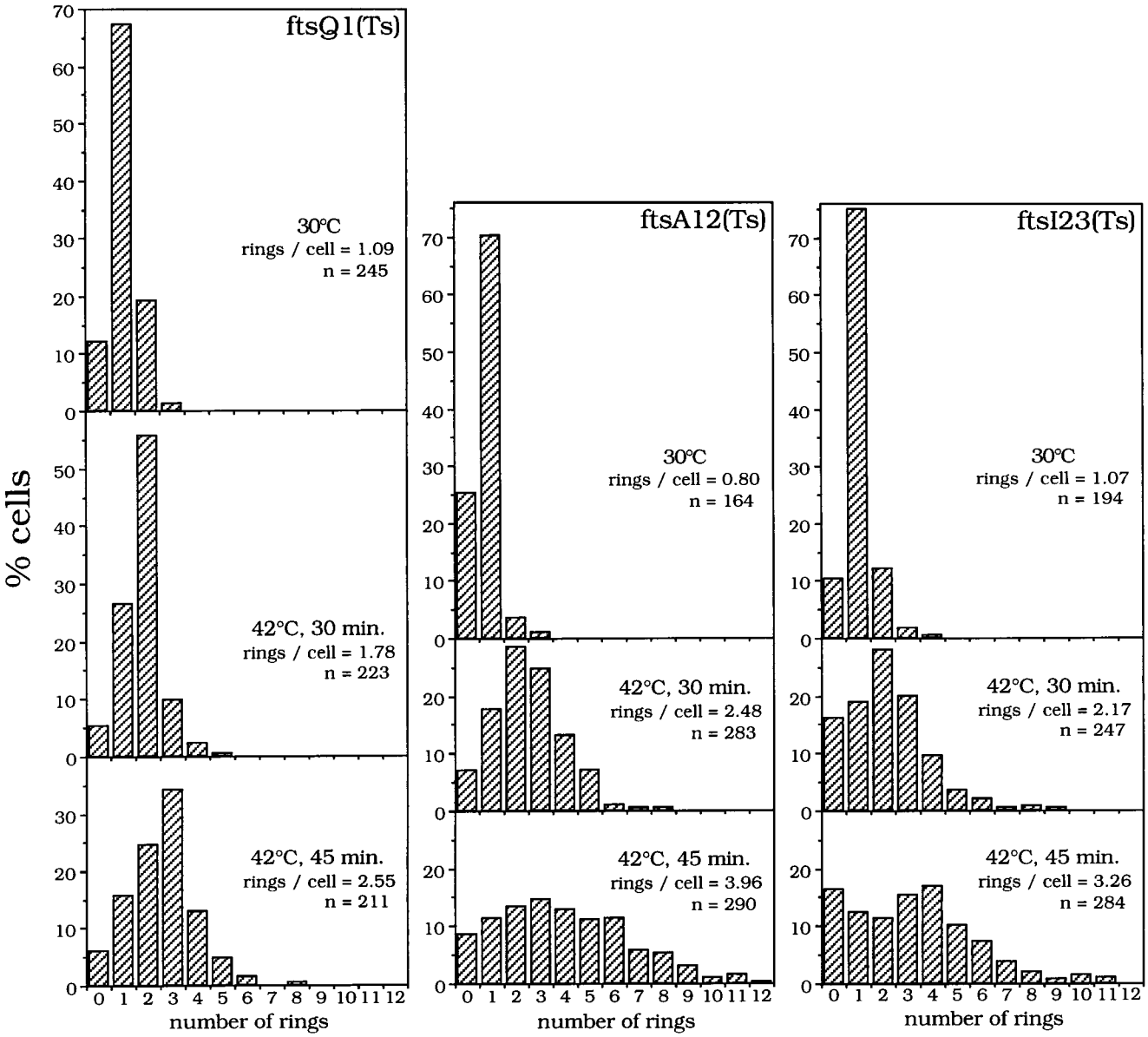

FIG. 7. Histograms indicating the number of Z rings per cell. The number of rings per cell was determined in cultures of the *fts* mutants shown in Fig. 6. The mutants are indicated in the graphs.

results indicate that in these mutants Z-ring formation leads to the abortive divisions seen as indented filaments or sausages when the *fts* mutations are combined with a spherical mutation. Thus, the Z ring cannot cause complete invagination of the septum or the cytoplasmic membrane when synthesis of the septal peptidoglycan is inhibited, as in the *ftsI23* mutant. Instead, blocking of peptidoglycan biosynthesis must block progression of the Z ring and may lead to destabilization of the ring.

We observed quantitative similarities in Z-ring formation in filaments arising as a result of *ftsA12*, *ftsI23*, and *ftsQ1* mutations. In all cases, the average number of rings increased with time to similar extents at the nonpermissive temperature and cells with various numbers of rings were similarly distributed. Thus, loss of either of these gene products had the same effect on Z-ring formation and distribution. It will be of interest to determine the effect of mutations in other *fts* genes on Z-ring formation. Of interest is *ftsW*, which acts as an early cell division gene on the basis of the morphology caused by combining an *ftsW* mutation with a spherical mutation (18). However, it should be noted that homologs of *ftsW*, like other *fts* genes, except *ftsZ*, have not been found in the genome of *Mycoplasma genitalium* (15) and therefore may not have a direct role in FtsZ localization. We would expect a gene with such a role to be conserved in all bacteria.

The function of *ftsA* is unknown; however, it has been linked to the function of *ftsZ* and *ftsI* (10, 13, 28). Thus, FtsA may act to link the Z ring to septal peptidoglycan biosynthesis. Interestingly, a homolog of *ftsA* was not observed in the genome of *M. genitalium*, which lacks peptidoglycan (15). Taken together, these results suggest that the function of *ftsA* is related to the biosynthesis of peptidoglycan and connects the Z ring to FtsI.

Interestingly, the proper ratio of FtsA to FtsZ is important for cell division to take place, indicating that these proteins interact (10, 13). The results presented here indicate that FtsA acts after FtsZ.

Our results indicate that the Z ring is able to form in the absence of *ftsQ*, *ftsA*, and *ftsI* functions. Other possibilities are that the rings formed in the absence of these *fts* functions represent leakiness of the *fts* mutations utilized or that the mutations lead to a protein that has lost a function required for division but not the ability to localize the Z ring. These possibilities seem unlikely, since all of the mutations we examined yielded similar qualitative and quantitative results. We do not understand the heterogeneity observed within cells from the same mutant. Thus, we see filaments with many Z rings, as well as filaments with no or few rings and the length of the filament is not a clear indicator of the number of rings. This may be due to Z-ring turnover (discussed below), death of some filaments, or a technical problem, such as incomplete fixation or partial disintegration of the filaments. However, we think it is important to stress the point that the majority of filaments have rings and in fact the majority have multiple rings.

At the permissive temperature or in wild-type cells, the Z ring is present during most of the cell cycle and disappears only as it is utilized. There are two possible outcomes for the rings at 42°C: either they are stable once formed because they are not used, or they are unstable, perhaps because of the lack of the other *fts* gene products. To try to decide between these possibilities, we calculated the number of rings expected at 42°C provided the rings are stable. This can be done from the doubling time at 42°C, which is approximately 25 min for each of the mutants. Thus, after one generation time, we would expect three (two new ones and the old one), and after two, we would expect seven (four new and three old). If the rings are unstable, we would expect two (only the new) after the first generation and four (again only the new) after the second. The average number of rings we observe (Fig. 7) is closer to the second calculation, indicating that the rings might be unstable. Z-ring instability at 30°C is apparent in the *ftsQ1*(Ts) mutant, in which approximately 20% of the cells have two rings. In such cells, the two rings symmetrically flank a centrally located indentation which does not have a ring. Since many of these cells have a deep midcell indentation, it suggests that a Z ring was present and initiated division but then aborted. Similar observations were made for the *ftsI23*(Ts) mutant grown at 30°C. Ring instability would also help explain the heterogeneity we observe in the number of rings per cell at the nonpermissive temperature. We will test this possibility in the future.

Since the Z ring can form in the absence of *ftsQ*, *ftsA*, and *ftsI* functions, these genes are unlikely to play a role in localization of the ring. Instead, one of the functions of the Z ring may be to recruit these and other *fts* gene products to the division site. The results obtained with wild-type cells, indicating a significant time between Z-ring formation and visible invagination, raise the possibility of regulation of the function of the Z ring once it is formed. For example, inhibitors of FtsA or FtsI could also stall the Z ring. However, known inhibitors, such as SulA and MinCD, act to prevent Z-ring formation (4; data not shown).

ACKNOWLEDGMENTS

We thank Kit Pogliano for providing a protocol for immunofluorescent staining.

This work was supported by Public Health Service grant RO1 GM29764.

REFERENCES

1. **Begg, K. J., and W. D. Donachie.** 1985. Cell shape and division in *Escherichia coli*: experiments with shape and division mutants. J. Bacteriol. **163:**615–622.
2. **Bi, E., and J. Lutkenhaus.** 1991. FtsZ ring structure associated with division in *Escherichia coli*. Nature (London) **354:**161–164.
3. **Bi, E., and J. Lutkenhaus.** 1992. Isolation and characterization of *ftsZ* alleles that affect septal morphology. J. Bacteriol. **174:**5414–5423.
4. **Bi, E., and J. Lutkenhaus.** 1993. Cell division inhibitors SulA and MinCD prevent formation of the FtsZ ring. J. Bacteriol. **175:**1118–1125.
5. **Bork, P., C. Sander, and A. Valencia.** 1994. An ATPase domain common to prokaryotic cell cycle proteins, sugar kinases, actin and hsp70 heat shock proteins. Proc. Natl. Acad. Sci. USA **89:**7290–7294.
6. **Botta, G. A., and J. T. Park.** 1981. Evidence for involvement of penicillin-binding protein 3 in murein synthesis during septation but not during cell elongation. J. Bacteriol. **145:**333–340.
7. **Bramhill, D., and C. M. Thompson.** 1994. GTP-dependent polymerization of *Escherichia coli* FtsZ protein to form tubules. Proc. Natl. Acad. Sci. USA **91:**5813–5817.
8. **Carson, M., J. Barondess, and J. Beckwith.** 1991. The FtsQ protein of *Escherichia coli*: membrane topology, abundance, and cell division phenotype due to overproduction and insertion mutations. J. Bacteriol. **173:**2187–2195.
9. **Casadaban, M.** 1976. Transposition and fusion of the *lac* gene to selected promoters in *E. coli* using bacteriophage λ and Mu. J. Mol. Biol. **104:**541–555.
10. **Dai, K., and J. Lutkenhaus.** 1992. The proper ratio of FtsZ to FtsA is required for cell division to occur in *Escherichia coli*. J. Bacteriol. **174:**6145–6151.
11. **Dai, K., Y. Xu, and J. Lutkenhaus.** 1993. Cloning and characterization of *ftsN*, an essential cell division gene in *Escherichia coli*, isolated as a multicopy suppressor of *ftsA12*(Ts). J. Bacteriol. **175:**3790–3797.
12. **de Boer, P., R. Crossley, and L. Rothfield.** 1992. The essential bacterial cell-division protein FtsZ is a GTPase. Nature (London) **359:**254–256.
13. **Dewar, S. J., K. J. Begg, and W. D. Donachie.** 1992. Inhibition of cell division initiation by an imbalance in the ratio of FtsA to FtsZ. J. Bacteriol. **174:**6314–6316.
14. **Erickson, H. P., D. W. Taylor, K. A. Taylor, and D. Bramhill.** 1996. Bacterial cell division protein FtsZ assembles into protofilament sheet and minirings, structural homologs of tubulin polymers. Proc. Natl. Acad. Sci. USA **93:**519–523.
15. **Fraser, C. M., J. D. Gocayne, O. White, et al.** 1995. The minimal gene complement of *Mycoplasma genitalium*. Science **270:**397–403.
16. **Harry, E. J., K. Pogliano, and R. Losick.** 1995. Use of immunofluorescence to visualize cell-specific gene expression during sporulation in *Bacillus subtilis*. J. Bacteriol. **177:**3386–3393.
17. **Huisman, O., and R. D'Ari.** 1981. An inducible DNA replication-cell division coupling mechanism of *Escherichia coli*. Nature (London) **290:**797–799.
18. **Khattar, M., K. J. Begg, and W. D. Donachie.** 1994. Identification of FtsW and characterization of a new *ftsW* division mutant of *Escherichia coli*. J. Bacteriol. **176:**7140–7147.
19. **Levin, P., and R. Losick.** 1996. Transcription factor SpoOA switches the localization of the cell division protein FtsZ from a medial to a bipolar pattern in *Bacillus subtilis*. Genes Dev. **10:**478–488.
20. **Lutkenhaus, J.** 1993. FtsZ ring in bacterial cytokinesis. Mol. Microbiol. **9:**404–409.
21. **Maddock, J., and L. Shapiro.** 1993. Polar location of the chemoreceptor complex in the *Escherichia coli* cell. Science **259:**1717–1723.
22. **Mukherjee, A., K. Dai, and J. Lutkenhaus.** 1993. *E. coli* cell division protein FtsZ is a guanine nucleotide binding protein. Proc. Natl. Acad. Sci. USA **90:**1053–1057.
23. **Mukherjee, A., and J. Lutkenhaus.** 1994. Guanine nucleotide assembly of FtsZ into filaments. J. Bacteriol. **176:**2754–2758.
24. **Nanninga, N.** 1991. Cell division and peptidoglycan assembly in *Escherichia coli*. Mol. Microbiol. **5:**791–795.
25. **RayChaudhuri, D., and J. T. Park.** 1992. *Escherichia coli* cell-division gene *ftsZ* encodes a novel GTP-binding protein. Nature (London) **359:**251–254.
26. **Spratt, B. G.** 1977. Temperature-sensitive cell division mutants of *Escherichia coli* with thermolabile penicillin-binding proteins. J. Bacteriol. **131:**293–305.
27. **Taschner, P. E., P. G. Huls, E. Pas, and C. L. Woldringh.** 1988. Division behavior and shape changes in isogenic *ftsZ*, *ftsQ*, *ftsA*, *pbpB*, and *ftsE* cell division mutants of *Escherichia coli* during temperature shift experiments. J. Bacteriol. **170:**1533–1540.
28. **Tormo, A., J. A. Ayala, M. A. de Pedro, and M. Vicente.** 1986. Interaction of FtsA and PBP3 proteins in the *Escherichia coli* septum. J. Bacteriol. **166:**985–992.
29. **Wang, X., and J. Lutkenhaus.** 1993. FtsZ protein of *Bacillus subtilis* is localized at the division site and has GTPase activity that is dependent upon FtsZ concentration. Mol. Microbiol. **9:**435–442.